IEEE Access
Multidisciplinary | Rapid Review | Open Access Journal

Received 16 May 2023, accepted 27 May 2023, date of publication 31 May 2023, date of current version 7 June 2023.

Digital Object Identifier 10.1109/ACCESS.2023.3281656

RESEARCH ARTICLE

Pulsed Laser Diode Based Wireless Power Transmission Application: Determination of Voltage Amplitude, Frequency, and Duty Cycle

HAYRI YIGIT[1], (Graduate Student Member, IEEE), AND ALI RIFAT BOYNUEGRI[1,2], (Member, IEEE)
[1]Department of Electrical Engineering, Yildiz Technical University, Istanbul 34220, Turkey
[2]Clean Energy Technologies Institute, Yildiz Technical University, Istanbul 34220, Turkey

Corresponding author: Ali Rifat Boynuegri (alirifat@yildiz.edu.tr)

This work was supported by the Scientific and Technological Research Council of Turkey under Project 121E564.

ABSTRACT Laser power transfer (LPT) is one of the leading technologies in long-distance power transmission with its advantages such as enabling high power transmission and suitability for mobile applications. The transmitter part, which includes the laser diode (LD) and the driving circuit, directly affects system efficiency. Continuous wave (CW) lasers are used in studies due to their high power and continuous radiation. However, one of the main disadvantage of the mentioned system is the high cost of LD. In this study, the use of pulsed LDs in LPT applications is proposed because of their small size and low cost. On the other hand, appropriate operating point of pulsed LD is missing information in the literature. In order to contribute literature with this information, pulsed LD is used for LPT, and the effects of driving voltage amplitudes, frequencies, and duty cycles are analyzed to demonstrate the importance of determining the appropriate operating point of the pulsed LD and the potential use of pulsed LDs in LPT.

INDEX TERMS Wireless power transfer, laser power transmission, laser diode, pulsed laser diode.

I. INTRODUCTION

Wireless power transmission (WPT) technology has seen significant improvements in recent years, enabling energy transfer without any physical or electrical connection between two points. This technology is becoming increasingly popular in consumer electronics, drone and robotic technologies. According to market research, the WPT market was valued at 9.53 billion USD in 2020 and is projected to reach 15.45 billion USD in 2028 [1]. WPT is particularly useful for fast, convenient charging of electric vehicles and mobile devices, and has many potential applications. While the technology is mainly applied in short-distance applications, researchers have also been studying long-distance transmission possibilities [2], [3]. Long-distance WPT is especially relevant in situations where cabling is not feasible or impractical, such as in mobile vessels, air and ground vehicles, or in WPT from space to earth or vice-versa [4], [5].

WPT involves sending power without any physical cables. There are several methods to do this, such as inductive power transfer (IPT), capacitive power transfer (CPT), microwave power transfer (MPT), and laser power transfer (LPT) [2]. Both IPT and CPT methods are highly efficient at transmitting high power over short distances, and are used in applications such as powering mobile phones, electric vehicles, and implantable biomedical devices [6], [7], [8], [9]. However, as the distance between the transmitter and receiver increases, the efficiency of the WPT decreases as the magnetic and electric fields weaken, and it may become impossible to transmit power at some point [10].

MPT and LPT are two prominent technologies in long-distance WPT. Both technologies have a long history, but recent advancements in semiconductor, optical, and microwave technologies have made them more viable options in recent years. One of the main applications for MPT is for

The associate editor coordinating the review of this manuscript and approving it for publication was Qi Li.

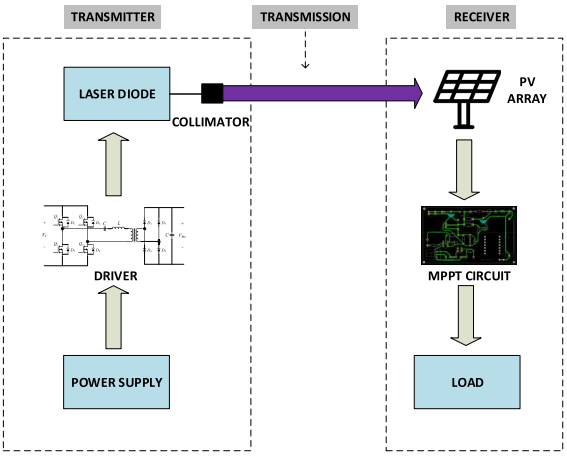

FIGURE 1. Schematic diagram of an LPT system.

long-distance power transmission from space to earth and powering mobile devices like drones, helicopters, and model airplanes [5], [11]. Although MPT is capable of transmitting power over long distances through the atmosphere using high-frequency microwaves, its main drawbacks include low system efficiency, difficulties in focusing microwaves to the receiving antenna, and increased cost due to the need for additional equipment to direct the microwaves [6], [12].

LPT technology is a promising option for wireless power transmission, particularly for mobile devices such as unmanned aerial vehicles and robots, as it allows for uninterrupted power transfer over several kilometers using a high-power density laser beam [13], [14]. Despite its low efficiency, LPT technology has some advantages over MPT, such as higher energy density and greater flexibility in applications [15].

The general layout of an LPT system is shown in Fig. 1, which consist of two main parts, the transmitter and the receiver. The transmitter converts electrical energy into a laser beam using a laser diode (LD), which is then directed towards the receiver via a collimating lens. At the receiver, the laser beam is converted back into electrical energy to power a load, drive a motor, or charge a battery. In order to ensure efficient conversion of the laser beam to electricity at the receiver, it is important to choose the right type of photovoltaic (PV) cell. There are various studies that investigate this aspect, including the effect of laser beam intensity and temperature on the PV, as well as the selection and development of suitable PV materials for different laser wavelengths [16], [17], [18]. For example, GaAs cells have been found to be suitable for wavelengths around 808 nm, while Si cells are ideal for the 900-976 nm range, which is common for LDs [19]. The receiver also includes global maximum power point tracking (MPPT), cell geometry, and different connection types of cells due to the Gaussian laser beam [19], [20], [21]. In addition to all these mentioned parts, the most crucial component of the system is the laser itself.

Different types of lasers can be used in an LPT system with each having its own advantages and disadvantages. In the early 2000s, lasers such as Nd:YAG and disk lasers were commonly used in LPT [21], [22], [23]. In [22], researchers were able to achieve power transmission of up to 1 km using a high-power, 1060 nm disk laser of 8 kW. Steinsiek et al. using a 5 W Nd:YAG laser were able to transfer power to a mini rover at a distance of about 80 m [23]. These types of lasers are suitable for long-range LPT due to their high power and good beam quality. However, their low efficiency in converting electrical energy to optical energy is a drawback and limits their use in LPT applications.

In recent years, LDs have emerged for LPT applications. They are highly efficient and compact, making them a popular choice in LPT. LDs are highly efficient, with typical power conversion efficiencies ranging from 30% to 50%, making them a cost-effective choice for high-power applications [19]. One of the critical characteristics of LD is the L/I curve, which plots the drive current applied to the laser against the output light intensity. This curve is used to determine the LD's operating point and threshold current. The threshold of the LD is affected by the LD's temperature, which increases exponentially with temperature. The efficiency of an LD is also derived from the L/I curve, and it falls off with increasing temperature. Pulsed L/I characteristics may also be acquired, and the rise in junction temperature causes an increase in threshold and a decrease in slope efficiency. The voltage drop across the LD is often acquired during electrical characterization, and it is largely invariant with temperature [25]. These LD characteristics have a significant impact on the LPT system, and understanding them is critical to developing an efficient and stable system. Understanding these characteristics and optimizing the operating point of the LD is critical to achieving high efficiency and reliable operation in LPT.

By using LDs in LPT systems, the overall efficiency of the system can be increased. This is because LDs are not only efficient at converting electrical energy into light, but they also emit light in a specific wavelength range that is well-matched to the PV cells used in the receiving end of the system. This results in higher PV efficiencies and overall system efficiency [18], [24]. Thanks to the technology of combining multiple LDs, the power output from each LD can be combined into a single laser beam with high power. Combining the outputs of multiple LDs into a single beam enables the achievement of high beam quality, brightness, and power density. This technology also allows for the adjustment of output power to meet the requirements of different systems [26].

The conversion efficiency of an LD is affected by the input current. The driver circuit for the LD is an important part of the system that can affect both the laser performance and overall system efficiency. Initially, linear current regulators were used to provide the low current ripple required for the LD [27]. However, the low efficiency and large size of linear current regulators made them less suitable for high-power

TABLE 1. Literature summary of LPT studies.

Reference	Laser Type	Pulsed Drive	Duty Cycle	Frequency	Amplitude	System Output Power (W)	System Efficiency (%)	Distance (m)
[21], [23]	Nd:YAG	×	×	×	×	19	NA	3
[22]	Disk	×	×	×	×	100	1.25	1000
[14], [18]	LD	×	×	×	×	9.7	11.6	100
[28]	LD	✓	×	×	×	0.75	2.5	NA
[15], [32]	LD	✓	✓ (40-100%)	×	×	3.2	8.85	0.35
This Study	LD	✓	✓ (5-35%)	✓ (5-20 kHz)	✓ (4.4-8.3 V)	0.2	7.76	0.5

* × indicates that the change of the relevant parameter was not examined in the related study.
** ✓ indicates that the change of the relevant parameter was examined in the related study.
*** NA indicates that the relevant data was not available in the study.

applications, leading to the development of switch mode power supplies [19]. Currently, LDs are commonly driven with DC-DC converters due to their low current ripple, high efficiency, and small size, along with filter structures at the output.

LDs can be operated in both continuous (CW) and pulsed mode for LPT application. CW LDs are often preferred for LPT due to their ability to provide uninterrupted power. Pulsed mode operation is typically used for communication and signaling, but it can also be used in LPT. In simple cases, pulsed LDs are used when both data transfer and power transfer are required [28]. A study have been conducted to examine the effect of different driving modes on CW LD performance and it was found that LDs have a higher conversion efficiency in pulsed mode compared to CW mode [15].

Table 1 shows the differences between the proposed study and the LPT studies in the literature. In contrast to existing literature, this study explores the impact of frequency and voltage variations on LD and LPT. As depicted in Table 1, the number of studies focusing on LPT with pulsed drive is limited and recent, with only one investigation considering the effect of duty cycle. However, none of these studies have examined the influence of frequency and amplitude. In this study, it is aimed to use pulsed LDs, which are more compact and cost-effective than CW lasers, for LPT applications. In pulsed mode operation, the same output power can be achieved at different amplitudes, duty cycles, and frequencies. Therefore, it is important to identify the optimal operating point where the output power and efficiency are high. To achieve this, the effects of frequency, duty cycle and voltage amplitude on LD and LPT are investigated by testing the LD at different frequencies, duty cycles and voltage levels. The main contributions of this research are as follows:

- Low-cost transmitter using pulsed LD in LPT application.
- Investigation of the effects of frequency, voltage, and duty cycle changes on LD performance and the power taken from the PV cell as a result of LPT.
- Determination of the appropriate operating point of the LD for LPT application.

The rest of the paper is structured as follows: The system description and modeling are discussed in Section II. Section III demonstrates the experimental setup and presents the results that we obtained from the experiments. Finally, Section IV presents the conclusion and future studies.

II. SYSTEM OVERVIEW

As discussed earlier, an LPT system typically has two parts: a transmitter and a receiver. In this section, the theoretical background and the methods used in the study are explained in detail for both the transmitter and receiver parts.

A. TRANSMITTER PART

LPT can be achieved both with a CW or intermittent laser beam. While CW mode may appear to be more appropriate for the purpose of the application, pulsed laser beams have their own advantages. First, pulsed LDs can achieve higher peak powers than CW LDs. This is because the pulse duration of a pulsed LD is much shorter than the period of the laser oscillation in a CW LD, allowing for a larger amount of energy to be stored and released in each pulse. Second, pulsed LDs have a higher tolerance for back reflections, which can cause damage to the LD. This is because the high peak power of the pulse can overcome the power of the reflected light. Third, pulsed LDs are more efficient at converting electrical power into optical power since the energy is concentrated in a shorter time period. Moreover, pulsed LDs offer advantages such as smaller size, and lower cost. However, pulsed LDs also have some disadvantages, such as a lower average power output and a higher complexity of the driving circuit.

Therefore, the choice between a pulsed LD and a CW LD depends on the specific application and the trade-off between peak power and average power. In this section, theoretical and mathematical comparison at these two technologies is provided. As shown in Fig. 2, CW lasers emit a constant, uninterrupted laser beam, while pulsed lasers emit intermittent beams. In pulsed emission, the average power is different from the peak power, so it is necessary to compare the energy or average power between the two emission types.

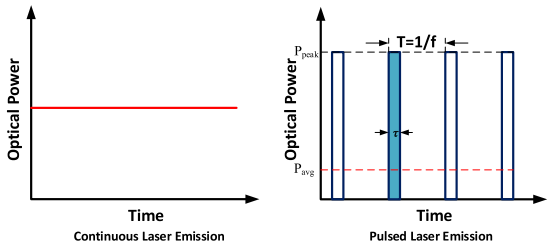

FIGURE 2. CW and pulsed laser emission.

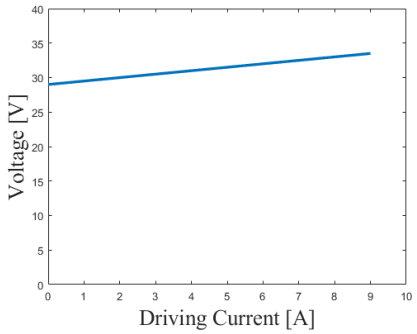

FIGURE 3. V-I characteristic curve of an LD.

The energy (E) in a period can be defined as the product of the peak power and the pulse width (τ) using the following equation

$$E = P_{peak}\tau \tag{1}$$

Average power (P_{avg}) can be calculated from the pulse energy divided by the period or multiplied by the frequency (f)

$$P_{avg} = \frac{E}{T} = Ef \tag{2}$$

The equation in (1) can be substituted into (2) to obtain the average power, which is the product of the peak power and the duty cycle (D). D is the ratio of the pulse width to the period. CW mode and pulse mode lasers can be compared when average power can be arranged as

$$P_{avg} = P_{peak}f\tau = \frac{P_{peak}\tau}{T} = P_{peak}D \tag{3}$$

Since LDs are current-driven devices, the output optical power (p_o) can be expressed depending on the LD current (i) [29]

$$p_o = \eta_d(i - I_{th}) \tag{4}$$

In this context, η_d represents the differential slope efficiency, and I_{th} represents the threshold current. These two values can be considered as constants as long as the temperature is kept constant, for the sake of simplicity.

The V-I characteristic curve of an LD is shown in Fig. 3. In a typical LD, the voltage across the LD remains nearly constant over a wide range of driving currents. This voltage-current relationship is due to the internal resistance of the LD, which is relatively low compared to the external circuit resistance. As a result, the voltage drop across the LD remains constant, and the driving current is the main factor that determines the output power of the LD [25]. Therefore, for the sake of simplicity in calculations, LD voltage V_{LD} can be considered constant. Thus, the electrical input power (p_i) can be computed using the following equation

$$p_i = V_{LD}i \tag{5}$$

From (4) and (5), the electro-optical conversion efficiency of an LD can be expressed as

$$\eta = \frac{p_o}{p_i} = \frac{\eta_d(i - I_{th})}{V_{LD}i} = \frac{\eta_d}{V_{LD}}(1 - \frac{I_{th}}{i}) \tag{6}$$

It can be seen from (6) that the conversion efficiency increases as the input current rises for a CW LD. However, these equations need to be rearranged for pulsed mode operation. The average optical output power (p_{o_p}) expressed for the pulsed LD can be described by using

$$p_{o\_p} = D\eta_d(i + I_{bias} - I_{th}) \tag{7}$$

where I_{bias} and D are the bias current and the ratio of the on-time to the period of PWM current. In a pulsed LD, the average optical power is equal to the peak optical power multiplied by the duty cycle (3). Meanwhile, for a CW LD, the optical power is defined in (4). In order to take into account, the additional I_{bias} that is added to the pulsed LD, we combined these two equations to obtain (7). The average electrical input power (p_{i_p}) and the conversion efficiency η_p can be found by the following equations

$$p_{i\_p} = \frac{1}{T}\int i_{LD}V_{LD}dt = V_{LD}(Di + I_{bias}) \tag{8}$$

$$\eta_p = \frac{p_{o\_p}}{p_{i\_p}} = \frac{D\eta_d(i + I_{bias} - I_{th})}{V_{LD}(Di + I_{bias})} \tag{9}$$

For the same optical output power, it will be seen that the efficiency of the LD increases at a lower duty cycle when different duty cycles are proportioned in the (7) [15].

The results show that the theoretical and experimental values are consistent until thermal losses reach a certain point. Above this point, the difference between the theoretical and experimental results increases. Also, LD is energized for a long time at low frequencies, which causes high thermal losses. However, since thermal modeling is not within the scope of this study, a coefficient called K_T is defined to model the thermal effects. This coefficient is generated empirically from the experimental data using a curve-fitting method. The coefficient K_T is a function of frequency and thermal losses. When the frequency is from the 2nd order and the thermal losses are from the 1st order, the simulation and experimental results overlap with an accuracy of about 85%. To account for the thermal effect, the thermal losses (p_T) of the LD are first calculated using the following equation

$$p_T = p_{i\_p} - p_{o\_p} \tag{10}$$

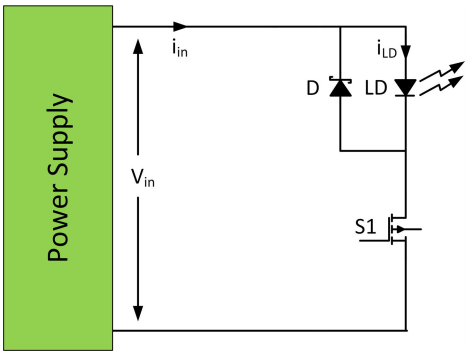

FIGURE 4. Block diagram of the LD test circuit.

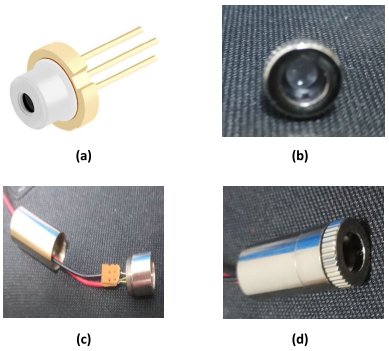

FIGURE 5. Placing the LD in the sheath, (a) LD, (b) Collimator lens, (c) Placing the LD in the heatsink, (d) Final LD with heatsink mounted and lens attached.

Therefore, K_T can be determined from experimental results using a curve fitting method to account for this effect by using

$$K_T = 0.6666 - 0.2887 * p_T + 0.09512 * f + 0.0006261 * p_T * f - 0.002809 * f^2 \quad (11)$$

The value of K_T varies based on the frequency (f) and thermal loss (p_T). The LD output power can be obtained by multiplying (7) with the K_T determined by the curve-fitting method to take into account the thermal effect

$$p_{o\_p} = D\eta_d(i + I_{bias} - I_{th}) * K_T \quad (12)$$

The circuit diagram of the test setup used to determine the optimal operating region of the LD is shown in Fig. 4. This setup includes an S1 MOSFET connected in series with the LD and a D Schottky diode connected in parallel. The power supply controls the voltage of the LD and provides the necessary power for the LD. The Schottky diode serves as a protection against overvoltage, reverse polarization, and electrostatic discharge as a clamping diode, as noted in references [30] and [31]. The MOSFET's role is to switch the LD on and off at a specific duty cycle and frequency. Programmable output regulated power supply was used that allowed us to control the output voltage with an accuracy of 1 mV. The circuit in the Fig. 4 is built. The LD is connected to the circuit with the help of connectors.

An LD seen in Fig. 5a with an instantaneous peak optical power of 125 W and a wavelength of 905 nm, which is packaged in a TO-56 case, was used. As per the manufacturer's specifications, this LD has a typical pulse duration of 100 ns. In this study, the LD was operated at a lower power level than its maximum, but at higher duty cycles, and active cooling was used to keep the temperature in check. The LD was placed in a heat-dissipating enclosure, known as a "sheath," to help remove the heat generated during the lasing process.

The process of placing the LD into the sheath is shown in Fig. 5. It's crucial that the laser beam is aligned correctly in the slot to ensure that it's transmitted perpendicular to the receiver. Additionally, the diameter of the collimated beam changes based on the distance between the lens and the LD, so it's important to adjust the lens distance to ensure that the entire laser beam falls on the PV cell for maximum power output.

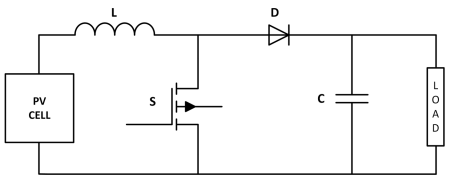

FIGURE 6. MPPT circuit.

B. RECEIVER PART

The receiver part of the proposed LPT system uses a Si cell. To ensure efficient conversion of the laser beam to electricity, it's crucial that the wavelength of the LD and the PV cell material are compatible. The energy of the photon directed to the PV cell must be greater than or equal to the band gap energy of the material. Since the energy of a photon is proportional to its frequency and thus to its wavelength, the PV cells respond to specific laser beam wavelengths that match the bandgap energies of the cell. The cutoff wavelength λ_c of the beam on the PV surface, E_g the band gap energy of the material, can be found by the formula below [18]

$$\lambda_c = \frac{1240}{E_g} \quad (13)$$

As the bandgap energy of Si is 1.12 eV, it is well-suited for a 905 nm laser beam. Additionally, research has shown that a Si cell has a high conversion efficiency at 905 nm, as seen in a graph of wavelength-PV conversion efficiency for different PV materials [19].

The voltage and current at the maximum power point (MPP) of a PV cell vary depending on the temperature T and the radiation G as in the following equations [32]

$$V_m = V_m(stc).ln(e + b.\Delta G).(1 - c.\Delta T) \quad (14)$$

$$I_m = I_m(stc).\frac{G}{G(stc)}.(1 + a.\Delta T) \quad (15)$$

In this case, stc stands for "Standard Test Conditions" and it means that the irradiance level is set to 1000 W/m^2 and the cell temperature is 25°C. The variables ΔT and ΔG

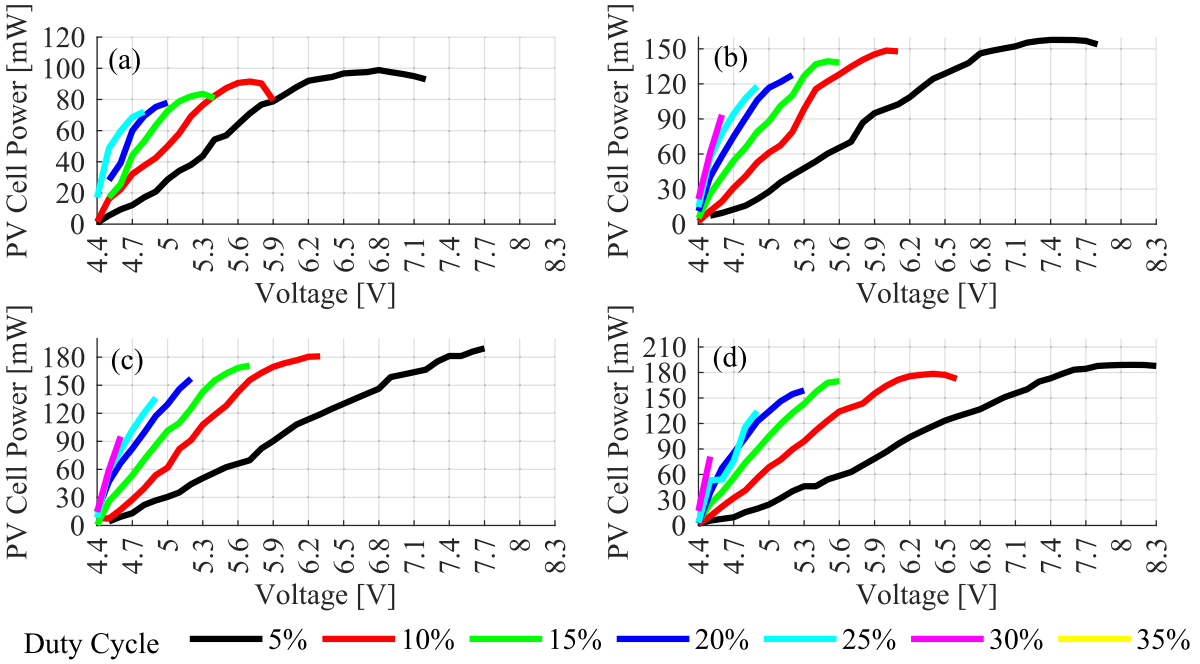

FIGURE 7. Simulation results of power obtained from a PV cell for four different frequencies (a) 5 kHz (b) 10 kHz (c) 15 kHz (d) 20 kHz.

represent the difference in temperature and irradiance from these standard conditions, respectively. Coefficients a and c are used to account for how changes in temperature affect the PV cell performance, while coefficient b is used to account for how changes in irradiance affect the PV cell performance.

To keep the efficiency of the PV cells high, it is important to keep the temperature of the cells as low as possible. This can be achieved by using a cooling system in the LPT system. Therefore, temperature can be ignored when analyzing the efficiency characteristics of the PV cell, assuming that the temperature does not change due to cooling.

Where S is the surface area of the PV cell, $p_{in_{pv}}$ is the average input power of the PV cell, $p_{o_{pv}}$ is the average output power of the PV cell, and the efficiency η_{pv} can be obtained as following

$$p_{in\_pv} = D.G.S \tag{16}$$

$$p_{o\_pv} = \frac{1}{T}\int_0^T (v_m.I_m)dt = D.V_m(stc).I_m(stc).\frac{G.ln(e+b.\Delta G)}{G(stc)} \tag{17}$$

$$\eta_{pv} = \frac{V_m(stc).I_m(stc)}{S.G(stc)}.ln[e+b.(\frac{p_{in\_pv}}{D.S} - G(stc))] \tag{18}$$

In this study, the receiver's role is not only to convert the optical power into electrical power to complete the power transmission but also to measure the performance of the system. The system's performance is determined by the PV output power and the overall system efficiency, η_{sys}, which is calculated using the following equation

$$\eta_{sys} = \eta_{LD}\eta_{pv} = \frac{p_{pv\_avg}}{p_{LD\_avg}} \tag{19}$$

where p_{pv_avg} is the average power obtained from the PV cell, and p_{LD_avg} is the power given from the LD input. In addition, to obtain stable and maximum power from this PV cell, an MPPT circuit has been created. To implement MPPT, we selected a boost converter topology, as shown in Fig. 6. This is because the PV voltage at the MPP is typically low. The values of the inductor (L) and capacitor (C) are 55 μH and 100 μF, respectively. The converter operates at a switching frequency of 31 kHz.

In order to determine the optimal operating point of the LD in the LPT application, MATLAB software was utilized for simulation purposes. The simulation incorporated equations mentioned in the manuscript, taking into account the defined LD electrical parameters such as the threshold current (0.6 A) and slope efficiency (3.5 W/A). Additionally, the simulation encompassed the PV parameters, including a radiation coefficient (b) of -0.0004, V_{mpp} of 0.581, and I_{mpp} of 9.28. The simulation involved varying duty cycle (5-35%), voltage (4.4 V to 8.3 V), frequency (5-20 kHz), and current data. By utilizing loops for each frequency value, the LD output power, PV output power, and overall system efficiency were obtained. In Fig. 7, PV output power is plotted for different frequency and duty cycles. Each graph corresponds to a different frequency, and each line within the graph corresponds to a different duty cycle. The graphs show that the power obtained from the PV increases up to a certain level, but beyond that level, no power can be obtained due to the thermal

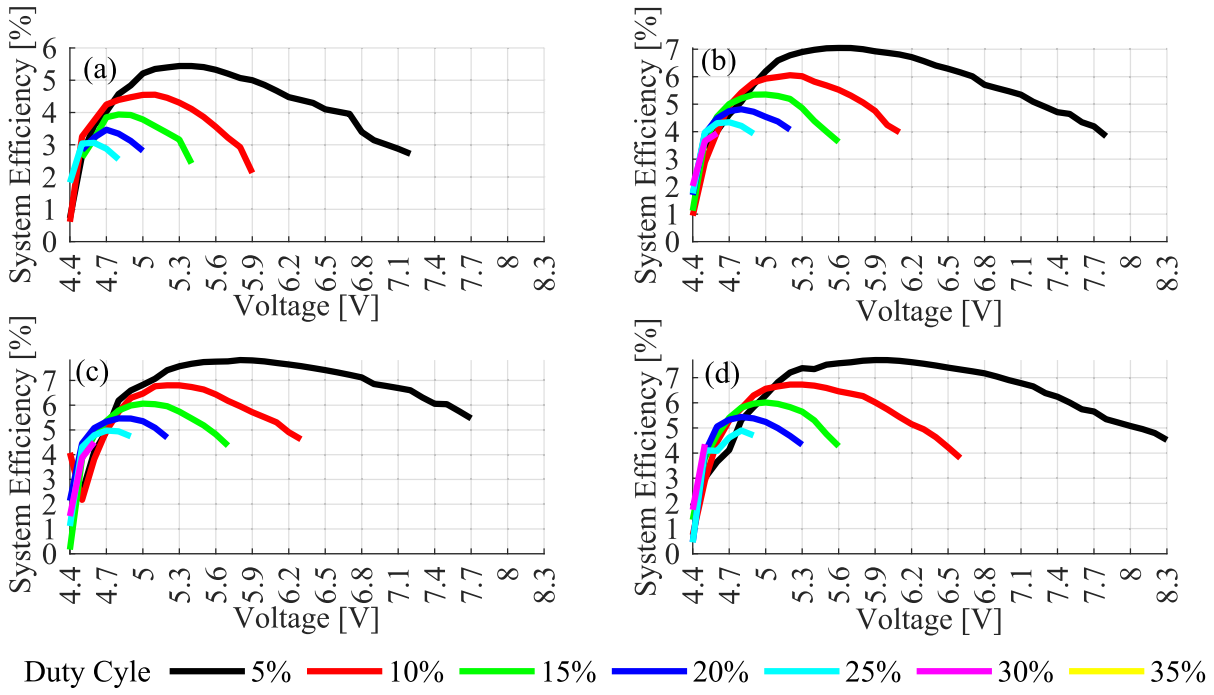

FIGURE 8. Simulation results of total system efficiency for four different frequencies (a) 5 kHz (b) 10 kHz (c) 15 kHz (d) 20 kHz.

resistance of the LD. The figure indicates that the PV output power is higher at lower duty cycles and higher frequencies.

Fig. 8 displays the efficiency curve, which is obtained by dividing the PV output power by the LD input power, at different frequencies and duty cycles. In the simulation results, the highest efficiency was achieved at low duty cycles and high frequencies. However, the efficiency rapidly drops after reaching the peak value. Theoretical efficiency was calculated as 8%.

III. EXPERIMENTAL SETUP AND RESULTS

To verify the proposed LPT technique which is explained theoretically in the section above, an experimental setup as shown in Fig. 9 is built. The goal of these experiments is to find the appropriate operating point of pulsed LD. The average output power and the efficiency are the main indicators of the system performance. For this reason, the results acquired from the experimental setup must demonstrate the effect of the duty cycle, frequency, and amplitude of the driving voltage of the pulsed LD separately. Here, DC power supply is used to control voltage amplitude and a DSP controller to adjust the LD's frequency and duty cycle.

TMS320F28379D LaunchPad of Texas Instruments was used as the controller. The MOSFETs in the LD driving and MPPT circuits were switched using PWM signals generated by the controller. By controlling the MOSFET with the PWM signal, the LD was driven and lasing in different conditions. Normally, alignment is one of the most important aspects of LPT practice. Because small fluctuations in the LD change the position of the laser beam on the receiving side too much. However, in this study, such a problem was not encountered since a sufficiently large PV cell was used and the distance was short. Also, the LD was aligned using a laser with a wavelength of 650 nm to prevent the beam from falling on the metallic conductors on the PV cell, to ensure the beam was always focused on the same spot, and to keep the lens alignment constant since the wavelength of the LD used for LPT is not in the visible region. The distance between the transmitter and receiver was fixed at 50 cm to eliminate distance effects. Finally, in order to get maximum power from the PV cell, the power was transferred to the load through the circuit following the MPP. The current and voltage values of the LD and PV cell were measured using the oscilloscope in the figure.

TABLE 2. Limitations of the experimental tests.

Parameter	Limitations
Voltage	4.4-8.3 V
Duty Cycle	5-35%
Frequency	5-20 kHz

Temperature measurements were made on the PV cell and LD, and all tests were conducted at constant ambient temperatures. The tests were conducted in a completely dark room to eliminate the effects of other sources of radiation. The equipment was arranged to ensure that radiation from other sources, such as power supplies, did not affect the results. Before starting the LD radiation, it was seen that the power values read on the oscilloscope were quite small (microwatts) and this value was accepted as zero.

The parameters and limitations used in determining the operating point of the pulsed LD are given in Table 2. The lower limit of the voltage is 4.4 V, which corresponds to

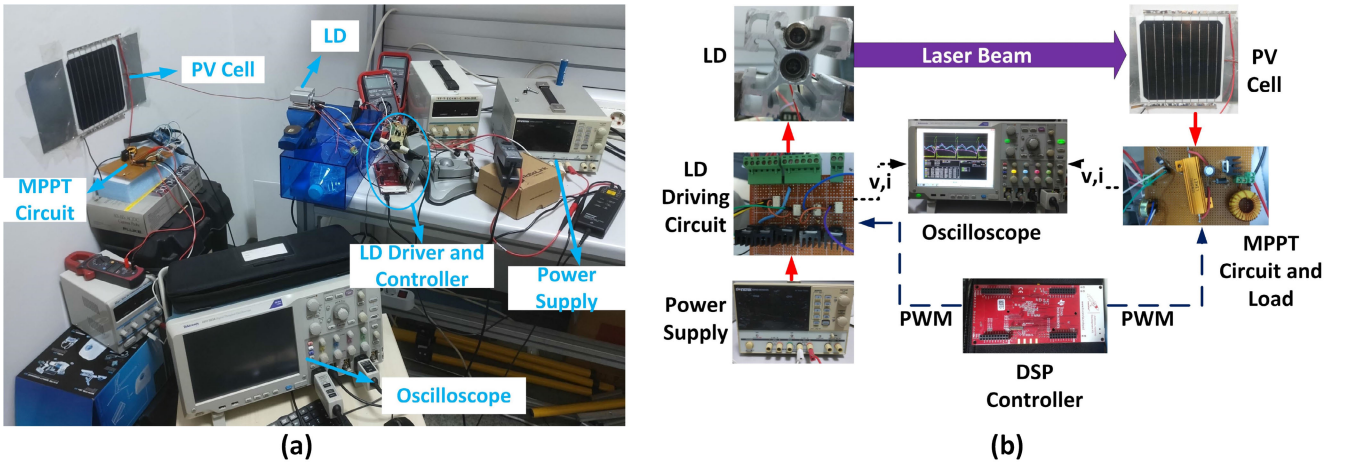

FIGURE 9. Schematic of the experimental setup: (a) complete overview of all components and (b) detailed connections between components.

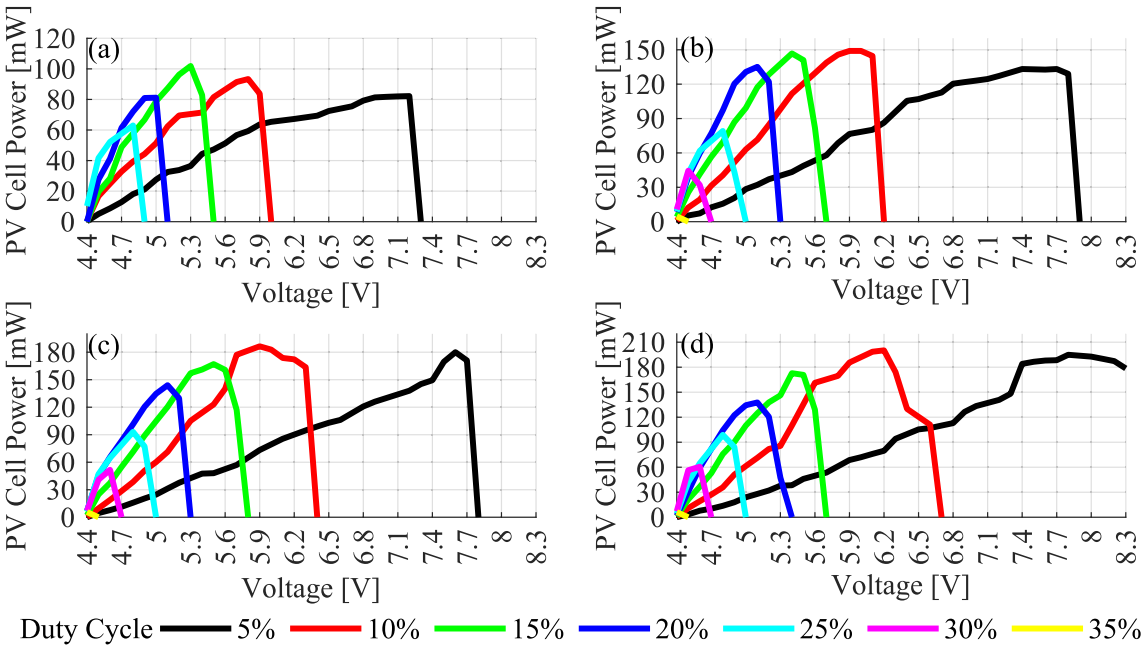

FIGURE 10. Voltage-varying PV cell power at a switching frequency of (a) 5 kHz (b) 10 kHz (c) 15 kHz (d) 20 kHz.

the threshold current value of the LD. The lower limit of the duty cycle is 5%, as the current cannot rise fast enough to exceed the threshold current value at duty cycles below this value. The upper limits for voltage and duty cycle are 8.3 V and 35%, respectively, because the LD overheats and cuts off radiation beyond these values. Tests were conducted both above and below the range of 5-20 kHz. However, the results obtained outside this range cannot be utilized due to the overheating of the LD, resulting in the absence of measurable power from the PV output. The goal of these tests was to determine the optimal operating point of the LD for the proposed laser power transmission system, and to examine the effects of the duty cycle, frequency, and voltage on the efficiency of the system.

A. EFFECTS OF VOLTAGE AMPLITUDE ON SYSTEM PERFORMANCE

In order to understand how the voltage level affects the performance of the LD and the LPT system, tests were conducted by keeping the duty cycle and frequency constant and incrementing the voltage by 0.1 V intervals. The results are presented below for each frequency separately. Fig. 10 shows the variation of the power obtained from the PV cell output depending on the voltage at 4 different frequencies and different duty cycles. In general, as the voltage increases, the power output from the PV cell also increases, but there is a point where the power output starts to decrease as the LD overheats and stops lasing. Depending on the equation in (3), the LD can operate in a wide voltage range at low duty cycles

such as 5-10%, while it operates in a narrow voltage range at high duty cycles such as 20-35%, and relatively low power is taken from the PV cell. This wide range reaches to 8.3 V at 20 kHz switching frequencies. As can be seen from the graphics, the highest power received from the PV cell at 10, 15, and 20 kHz was obtained at a voltage value in the middle of the voltage range at 10% duty cycle. The highest power received from the PV cell at only 5 kHz was obtained at a relatively low voltage value of 15% duty cycle.

In Fig. 10a, the graph shows the relationship between the power obtained from the PV cell output and the voltage at a switching frequency of 5 kHz, with data points for 5 different duty cycles. At this frequency, the highest power from the PV cell was 101.9 mW at a voltage of 5.3 V and a duty cycle of 15%. It can be seen that at lower duty cycles, the LD can operate over a wider range of voltages, but at higher duty cycles, the range is more narrow and the power taken from the PV cell is relatively lower. Variation of PV cell power depending on LD voltage at 10 kHz switching frequency is given in Fig. 10b. 4.65 mW is taken at 4.4 V LD voltage at 35% duty cycle at 10 kHz. While LD emits laser beam under the highest voltage of 7.3 V at 5 kHz switching frequency, it emits laser beam up to 7.8 V at 10 kHz. With 149 mW taken from the PV cell, the highest power was obtained under 5.9 V voltage at 10% duty cycle. Compared to the highest power value obtained at 5 kHz, approximately 50% more power, lower duty cycle, taken under higher voltage. It can be seen from Fig. 10c that the LD operating voltage rises to 7.8 V when the switching frequency of 15 kHz is increased. The highest power obtained from the PV cell at the relevant frequency value was obtained at a 10% duty cycle, 5.9 V voltage condition. In Fig. 10d, the graph shows the relationship between the power obtained from the PV cell output and the voltage at a switching frequency of 20 kHz, with data points for 7 different duty cycles. At this frequency, the highest power from the PV cell was 200.2 mW at a voltage of 6.2 V and a duty cycle of 10%.

B. EFFECTS OF DUTY CYCLE ON SYSTEM PERFORMANCE

In order to examine the effect of duty cycle on the performance of the LD and LPT, two different voltage levels were chosen for the tests. The first voltage level, 4.5 V, was selected because it allows the LD to operate at a higher duty cycle range, providing a wider range of duty cycle operation to observe. At the second voltage level, 5.3 V, the LD operates at lower duty cycles, but an average PV cell power is still obtained. This allows for an analysis of how the duty cycle affects the performance of the system at different voltage levels.

In Fig. 11, the power obtained from the PV cell is shown at different duty cycles and frequencies while operating the LD at 4.5 V. As seen in the figure, the power increases up to a certain point as the duty cycle increases. However, as the duty cycle increases further, the power decreases due to the increase in the temperature of the LD, resulting in the LD not lasing at all. The highest power from the PV cell is achieved

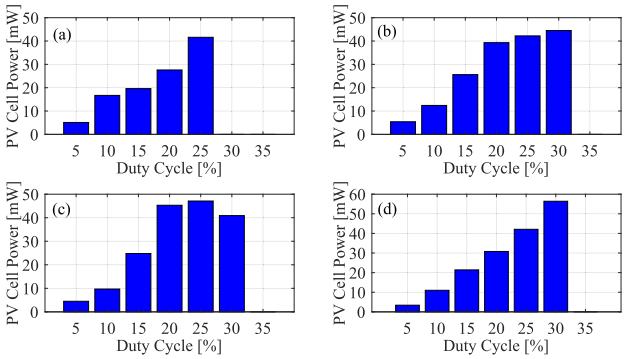

FIGURE 11. Duty cycle-varying PV cell power at 4.5 V and a switching frequency of (a) 5 kHz (b) 10 kHz (c) 15 kHz (d) 20 kHz.

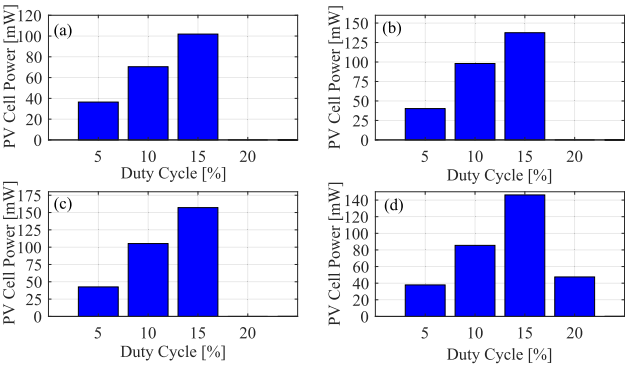

FIGURE 12. Duty cycle-varying PV cell power at 5.3 V and a switching frequency of (a) 5 kHz (b) 10 kHz (c) 15 kHz (d) 20 kHz.

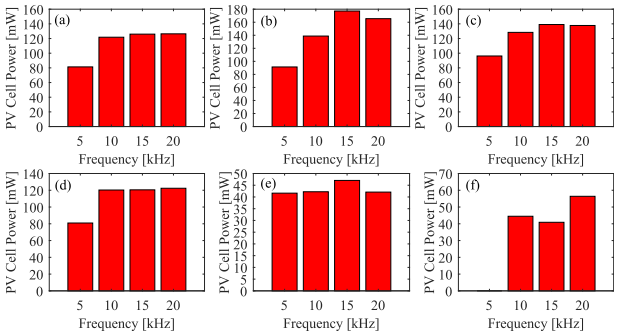

FIGURE 13. The power values taken from the PV cell depending on the frequency in different conditions.

at 25% duty cycle at 5 kHz and 15 kHz, at 30% duty cycle at other frequencies.

In Fig. 12, the effect of changing the duty cycle on the power output of the PV cell is shown while operating at different frequencies under a voltage of 5.3 V. The voltage level is higher than in the previous situation, the range of duty cycles that the LD can operate under 5.3 V has decreased. At this voltage level, the power obtained from the PV increases up to a certain duty cycle and then decreases. The highest power received from the PV cell at this voltage level was 157.1 mW, as seen in Fig. 12c, and was obtained at a frequency of 15 kHz and a duty cycle of 15%.

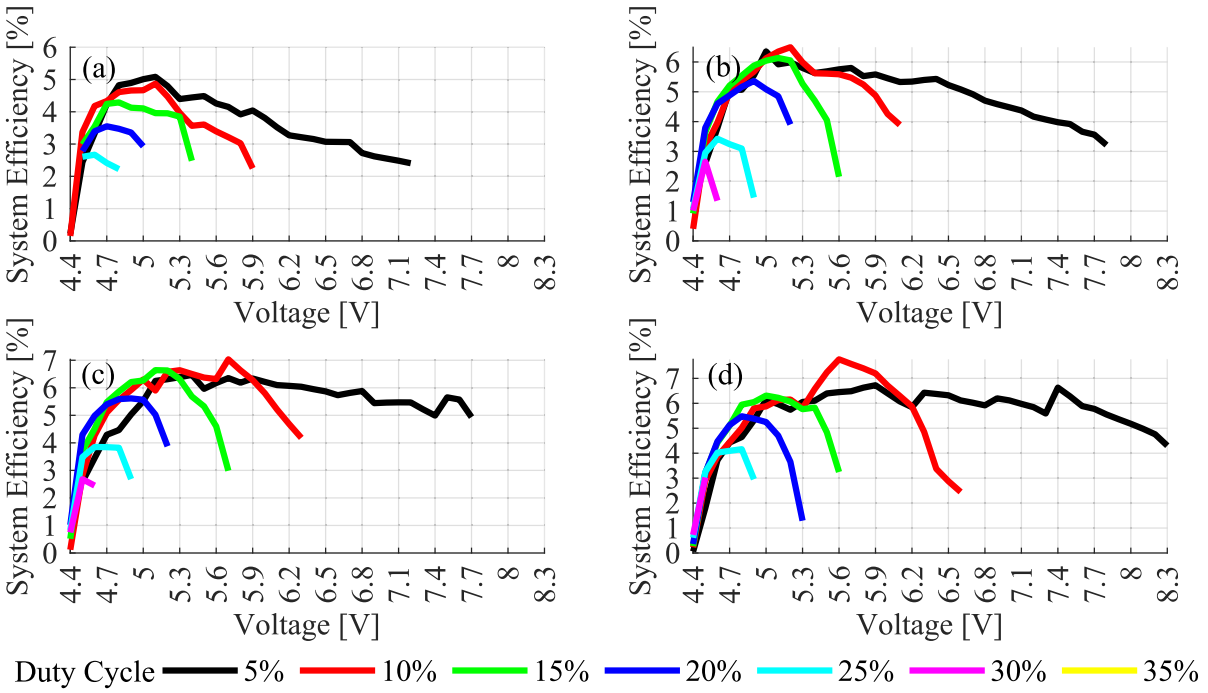

FIGURE 14. Total system efficiency of (a) 5 kHz (b) 10 kHz (c) 15 kHz (d) 20 kHz.

The duty cycle of the LD has a direct impact on the power output of the PV. Specifically, a higher duty cycle results in a longer period of light emission from the LD, which can lead to higher light intensity and therefore higher power output from the PV. However, it is important to note that the relationship between the duty cycle and power output is affected by temperature, which can limit the working range of the LD. Therefore, maintaining a constant temperature is crucial for achieving high power output from the PV, especially in space applications where temperature control is critical. In our tests under constant ambient conditions, designing a cooling system that will keep the temperature of both PV and LD constant will be positive in terms of efficiency. To this end, cooling systems such as water cooling or thermoelectric cooling can be employed to regulate the temperature and ensure consistently high performance.

C. EFFECTS OF FREQUENCY ON SYSTEM PERFORMANCE

In order to examine the effect of frequency change on the performance of the LPT system, the duty cycle and voltage were kept constant and the frequency was varied. The voltage level at which the highest possible power was taken from the PV cell was chosen for each frequency and duty cycle. The results, shown in Fig. 13, demonstrate the power values obtained from the PV cell depending on the frequency at different duty cycles (5-10-15-20-25-30%). Voltage levels are 6.9 V in Fig 13(a), 5.7 V in (b), 5.2 V in (c), 4.9 V in (d), 4.5 V in (e) and (f). These voltage levels are the highest voltage levels at which power is taken from the PV cell at all frequencies at the relevant duty cycle. At 10% duty cycle and 5.7 V voltage condition, the highest power received from the PV cell was measured as 177.2 mW at 15 kHz switching frequency. At 15% duty cycle 5.2 V voltage level, the highest power received from the PV cell is 139.1 mW at 15 kHz switching frequency, while it is 137.8 mW and 128.4 mW at 20 kHz and 10 kHz, respectively. When the duty cycle is increased to 20%, about 120 mW of power is obtained from the PV cell at 10, 15 and 20 kHz switching frequencies under 4.9 V voltage, while 80.95 mW is acquired at 5 kHz. Maximum power from the PV cell is 47.05 mW at a switching frequency of 15 kHz with a duty cycle of 25% and a voltage of 4.5 V. In this condition, more than 40 mW of power was taken from PV cell at other frequency values. Finally, the highest power obtained from the PV cell at 30% duty cycle, 4.5 V voltage was measured as 56.4 mW at 20 kHz switching frequency.

As can be seen from the figures, the highest power values obtained from the PV cell at the same voltage and duty cycle were taken at 15 and 20 kHz switching frequencies. At only 4.5 V voltage, 25% duty cycle, and 5 kHz frequency, the PV cell received power close to the values in other frequencies. Except for that condition, the power received from the PV cell is significantly lower at a 5 kHz switching frequency compared to other frequencies. As explained in the revised Section II of the paper, when the LD is energized for a long time at low frequencies, thermal losses are higher, and this affects the efficiency. However, it should also be noted that LD has been tested at higher frequencies, but it performed poorly at those frequencies, and enough power could not be transmitted. Therefore, it cannot be said that there is a complete linear relationship between frequency and PV power.

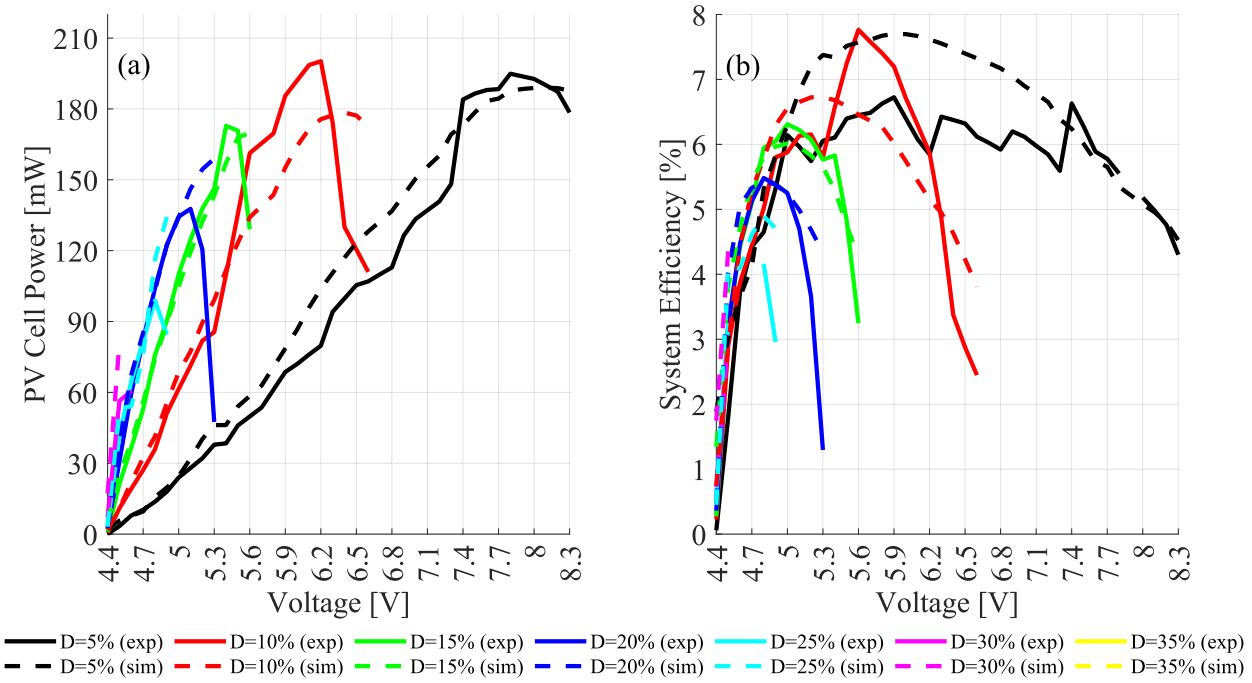

FIGURE 15. Comparison of simulation and experimental results at 20 kHz switching frequency (a) PV power (b) efficiency.

D. SYSTEM EFFICIENCY

Fig. 14 shows the end-to-end system efficiency, which is calculated by dividing the power obtained from the PV output shown in Fig. 10 by the LD input power. This efficiency metric provides a measure of how effectively the system is converting the energy from the PV source to power the LD and can be used to evaluate the overall performance of the system. The system achieved its highest efficiency of 7.76% at a frequency of 20 kHz, duty cycle of 10%, and voltage of 5.6 V. Upon examining the figures, it can be observed that the efficiency levels are generally similar at duty cycles of 5%, 10%, and 15%. Furthermore, an increase in frequency appears to have a positive impact on the system's efficiency.

Fig. 15a illustrates how the power received from the PV cell varies at a switching frequency of 20 kHz. The reason why we chose to compare at 20 kHz is that it provides the highest power and efficiency, and we didn't want to over-stretch the paper. The solid lines represent the experimental results, while the dotted lines depict the simulation results. From the figure, it's evident that the graph overlaps, indicating that the theoretical analysis is experimentally verified.

Fig. 15b depicts how the system's end-to-end efficiency varies at a switching frequency of 20 kHz. The solid lines represent the experimental results, while the dotted lines show the simulation results. The experimental and simulation results are consistent with each other, except for a specific region at a 10% duty cycle.

IV. CONCLUSION

LPT, a method of wireless power transmission using LDs, has many advantages such as electrical insulation and flexibility. This study focused on using pulsed mode LDs in LPT and investigated how varying the voltage, frequency, and duty cycle affects the performance of the system. It was observed that when the frequency and duty cycle are kept constant, increasing the voltage leads to an increase in power from the PV cell up to a certain point, after which it decreases suddenly. Similarly, when the voltage and frequency are kept constant, increasing the duty cycle leads to an increase in power from the PV cell up to a certain point, after which it decreases with the decrease of the optical power at the LD output due to heating. The study also found that higher PV cell power was obtained at higher switching frequencies of 15 and 20 kHz. The highest power obtained from the PV cell was 200.2 mW when 3.41 W was applied to the LD at 20 kHz switching frequency, 10% duty cycle, and 6.2 V voltage. Overall, the study emphasized the importance of determining the appropriate operating point of the pulsed LD.

As further work, future studies will focus on optimizing the alignment and developing control systems to maintain power transfer efficiency in case of a moving object.

ACKNOWLEDGMENT

The authors would like to thank the Scientific and Technological Research Council of Turkey for its financial support.

REFERENCES

[1] Verified Market Research. *Wireless Power Transmission Market Size and Forecast*. 2022. Accessed: Dec. 13, 2022. [Online]. Available: https://www.verifiedmarketresearch.com/product/wireless-power-transmission-market/

[2] A. Triviño, J. M. González-González, and J. A. Aguado, "Wireless power transfer technologies applied to electric vehicles: A review," *Energies*, vol. 14, no. 6, p. 1549, Jan. 2021, doi: 10.3390/en14061547.

[3] L. Xie, Y. Shi, Y. T. Hou, and A. Lou, "Wireless power transfer and applications to sensor networks," *IEEE Wireless Commun.*, vol. 20, no. 4, pp. 140–145, Aug. 2013, doi: 10.1109/MWC.2013.6590061.

[4] M. N. Boukoberine, Z. Zhou, and M. Benbouzid, "A critical review on unmanned aerial vehicles power supply and energy management: Solutions, strategies, and prospects," *Appl. Energy*, vol. 255, Dec. 2019, Art. no. 113823.

[5] B. Strassner and K. Chang, "Microwave power transmission: Historical milestones and system components," *Proc. IEEE*, vol. 101, no. 6, pp. 1379–1396, Jun. 2013, doi: 10.1109/JPROC.2013.2246132.

[6] J. Dai and D. C. Ludois, "A survey of wireless power transfer and a critical comparison of inductive and capacitive coupling for small gap applications," *IEEE Trans. Power Electron.*, vol. 30, no. 11, pp. 6017–6029, Nov. 2015, doi: 10.1109/TPEL.2015.2415253.

[7] J. Zhu, Y. Ban, R. Xu, and C. C. Mi, "An NFC-connected coupler using IPT-CPT-combined wireless charging for metal-cover smartphone applications," *IEEE Trans. Power Electron.*, vol. 36, no. 6, pp. 6323–6338, Jun. 2021, doi: 10.1109/TPEL.2020.3036459.

[8] C. C. Mi, G. Buja, S. Y. Choi, and C. T. Rim, "Modern advances in wireless power transfer systems for roadway powered electric vehicles," *IEEE Trans. Ind. Electron.*, vol. 63, no. 10, pp. 6533–6545, Oct. 2016, doi: 10.1109/TIE.2016.2574993.

[9] A. I. Al-Kalbani, M. R. Yuce, and J. Redouté, "A biosafety comparison between capacitive and inductive coupling in biomedical implants," *IEEE Antennas Wireless Propag. Lett.*, vol. 13, pp. 1168–1171, 2014, doi: 10.1109/LAWP.2014.2328375.

[10] K. Ramalingam and C. S. Indulkar, "Overview of plug-in electric vehicle technologies," in *Plug in Electric Vehicles in Smart Grids: Integration Techniques*. Singapore: Springer, 2015, pp. 1–32.

[11] S. Sasaki, K. Tanaka, and K.-I. Maki, "Microwave power transmission technologies for solar power satellites," *Proc. IEEE*, vol. 101, no. 6, pp. 1438–1447, Jun. 2013, doi: 10.1109/JPROC.2013.2246851.

[12] M. Shidujaman, H. Samani, and M. Arif, "Wireless power transmission trends," in *Proc. Int. Conf. Informat., Electron. Vis. (ICIEV)*, May 2014, pp. 1–6, doi: 10.1109/ICIEV.2014.6850770.

[13] Y. Lim, Y. W. Choi, and J. Ryoo, "Study on laser-powered aerial vehicle: Prolong flying time using 976 nm laser source," in *Proc. Int. Conf. Inf. Commun. Technol. Converg. (ICTC)*, Oct. 2021, pp. 1220–1225, doi: 10.1109/ICTC52510.2021.9621037.

[14] N. Kawashima and K. Takeda, "Laser energy transmission for a wireless energy supply to robots," in *Robotics and Automation in Construction*, vol. 10. London, U.K.: IntechOpen, 2008, pp. 373–380. [Online]. Available: https://www.intechopen.com/chapters/5576

[15] W. Zhou and K. Jin, "Efficiency evaluation of laser diode in different driving modes for wireless power transmission," *IEEE Trans. Power Electron.*, vol. 30, no. 11, pp. 6237–6244, Nov. 2015, doi: 10.1109/TPEL.2015.2411279.

[16] R. Mason, "Feasibility of laser power transmission to a high-altitude unmanned aerial vehicle," RAND Corp., Santa Monica, CA, USA, Tech. Rep., TR-898-AF, 2011.

[17] N. Singh, C. K. F. Ho, Y. N. Leong, K. E. K. Lee, and H. Wang, "InAlGaAs/InP-based laser photovoltaic converter at ∼ 1070 nm," *IEEE Electron Device Lett.*, vol. 37, no. 9, pp. 1154–1157, Sep. 2016, doi: 10.1109/LED.2016.2591015.

[18] T. He, S. H. Yang, H. Y. Zhang, C. M. Zhao, Y. C. Zhang, P. Xu, and M. Á. Muñoz, "High-power high-efficiency laser power transmission at 100 m using optimized multi-cell GaAs converter," *Chin. Phys. Lett.*, vol. 31, no. 10, pp. 1042031–1042035, 2014.

[19] K. Jin and W. Zhou, "Wireless laser power transmission: A review of recent progress," *IEEE Trans. Power Electron.*, vol. 34, no. 4, pp. 3842–3859, Apr. 2019, doi: 10.1109/TPEL.2018.2853156.

[20] W. Zhou, K. Jin, and R. Zhang, "A fast-speed GMPPT method for PV array under Gaussian laser beam condition in wireless power transfer application," *IEEE Trans. Power Electron.*, vol. 37, no. 8, pp. 10016–10028, Aug. 2022, doi: 10.1109/TPEL.2022.3155726.

[21] U. Ortabasi and H. Friedman, "Powersphere: A photovoltaic cavity converter for wireless power transmission using high power lasers," in *Proc. IEEE 4th World Conf. Photovoltaic Energy Conf.*, May 2006, pp. 126–129, doi: 10.1109/WCPEC.2006.279380.

[22] D. E. Becker, R. Chiang, C. C. Keys, A. W. Lyjak, J. A. Nees, M. D. Starch, C. Phipps, K. Komurasaki, and J. Sinko, "Photovoltaic-concentrator based power beaming for space elevator application," in *Proc. AIP Conf.*, 2010, pp. 182–271.

[23] F. Steinsiek, "Wireless power transmission experiment as an early contribution to planetary exploration missions," in *Proc. 54th Int. Astron. Congr. Int. Astron. Fed., Int. Acad. Astronaut., Int. Inst. Space Law*, Sep. 2003, pp. 169–176.

[24] D. E. Raible, "High intensity laser power beaming for wireless power transmission," M.S. thesis, Dept. Elect. Comput. Eng., Cleveland State Univ., Cleveland, OH, USA, May 2008.

[25] T. Hertsens. *An Overview of Laser Diode Characteristics*. Accessed: Mar. 10, 2023. [Online]. Available: https://rb.gy/jcdivi

[26] H. Liu, Y. Zhang, Y. Z. Hu Tse, and J. Wu, "Laser power transmission and its application in laser-powered electrical motor drive: A review," *Power Electron. Drives*, vol. 6, no. 1, pp. 137–184, Sep. 2021, doi: 10.2478/pead-2021-0010.

[27] F.-Z. Chen, Y.-C. Song, and F.-S. Ho, "An efficiency improvement driver for master oscillator power amplifier pulsed laser systems," *Processes*, vol. 10, no. 6, p. 1197, Jun. 2022.

[28] Y. Wang, C. Zhao, L. Zhang, Z. Zhang, and H. Zhang, "Hybrid pulse-width-modulation-based simultaneous wireless laser information and power transfer system using PWM sampling," *Opt. Commun.*, vol. 515, Jul. 2022, Art. no. 128232, doi: 10.1016/j.optcom.2022.128232.

[29] P. V. Mena, J. J. Morikuni, S.-M. Kang, A. V. Harton, and K. W. Wyatt, "A simple rate-equation-based thermal VCSEL model," *J. Lightw. Technol.*, vol. 17, no. 5, pp. 865–872, May 1, 1999, doi: 10.1109/50.762905.

[30] M. Zbik and P. Z. Wieczorek, "Versatile subnanosecond laser diode driver," in *Proc. SPIE*, vol. 10031, 2016, pp. 366–374.

[31] C. Hu, S. Qin, and X. Wang, "An extremely fast and high-power laser diode driver module," in *Proc. SPIE*, vol. 5628, 2005, pp. 12–17.

[32] W. Zhou, K. Jin, M. Wang, and Q. Wu, "Efficiency evaluation of laser based wireless power transmission system," in *Proc. IEEE Appl. Power Electron. Conf. Expo. (APEC)*, Mar. 2020, pp. 3147–3150, doi: 10.1109/APEC39645.2020.9124110.

HAYRI YIGIT (Graduate Student Member, IEEE) was born in Konya, Turkey, in 1997. He received the B.Sc. and M.Sc. degrees from Yildiz Technical University (YTU), Istanbul, Turkey, in 2020 and 2022, respectively, where he is currently pursuing the Ph.D. degree with the Department of Electrical Engineering. He is also a Research Assistant with the Department of Electrical Engineering, YTU. His current research interests include laser wireless power transmission and renewable energy systems.

ALI RIFAT BOYNUEGRI (Member, IEEE) was born in Istanbul, Turkey, in 1986. He received the B.Sc., M.Sc., and Ph.D. degrees from Yildiz Technical University, Istanbul, in 2008, 2010, and 2014, respectively, all in electrical engineering. He is currently an Assistant Professor with the Electrical Engineering Department, Yildiz Technical University. Prior to this position, he was with the University of Akron, Akron, OH, USA, for postdoctoral studies. His current research interests include alternative/renewable energy sources, electric vehicles, smart grids, predictive maintenance, power quality, and reactive power compensation. He is serving as a reviewer for IEEE Access, IEEE Transactions on Power Electronics, and IEEE Transactions on Transportation Electrification.